AR-004-264

DEPARTMENT OF DEFENCE

DEFENCE SCIENCE AND TECHNOLOGY ORGANISATION

ELECTRONICS RESEARCH LABORATORY

TECHNICAL MEMORANDUM

ERL-0346-TM

USE OF A LASER DIODE AS A SOURCE IN A BRAGG CELL SPECTRUM ANALYSER

C.I. Chessell

S U M M A R Y

The effects of using a solid state laser diode as the light source in an acousto-optic spectrum analyser are considered. Concentration is on high resolution analysers for use at communications frequencies. Recent developments in laser diode fabrication are summarised; key characteristics limiting performance are the spectral and spatial characteristics of the laser beam. The effects on analyser resolution and dynamic range are modelled and techniques proposed to improve performance.

POSTAL ADDRESS: Director, Electronics Research Laboratory,
Box 2151, GPO, Adelaide, South Australia, 5001.

TABLE OF CONTENTS

LIST OF FIGURES

5. Emission spectrum of general optronics laser diode GOLS-1/TB47 showing spontaneous emission. Laser output 3.9 mW, spectrometer bandpass 0.1 nm (from reference 1)

6. Typical far-field patterns of the HLP-1000 laser diodes parallel and perpendicular to the junction plane(ref.2)

7. Typical light versus current characteristics for the Hitachi HLP-1000 series laser diodes(ref.2)

8. Dominant lasing mode dependence on temperature and current for C^3 laser diode. Solid lines indicate mode hop boundaries; dashed line indicates better than 100:1 peak-to-sidelobe region (from reference 12)

9. Basic acousto-optic spectrum analyser

10. Model output, CW signal, 45 MHz, flat aperture weighting, 50 μs duration

11. Model output, CW signal, 45 MHz, flat aperture weighting, 10 μs duration

12. Gaussian laser intensity profiles for various values of the parameter T

13. Normalised AO spectrum analyser performance with Gaussian aperture weighting for various Gaussian parameter values. Input: CW signal, 45 MHz

14. Beam spread factor (3 dB) as a function of Gaussian beam truncation ratio T. Input: CW signal, 45 MHz

15. Available dynamic range as a function of Gaussian beam truncation ratio T for various pixel separations from "wanted" frequency pixel. Input: CW signal, 45 MHz

16. Intensity loss with respect to uniform aperture illumination as a function of the Gaussian beam truncation ratio T. Input: CW signal, 45 MHz

17. Intensity profiles used to test effect of variations from Gaussian

18. Model output, CW signal, 45 MHz, aperture intensity weighting curves A, B and C of figure 17

19. Beam apodisation device

20. Variation of signal ratio Sn/So with nearest neighbour pixel number for the case of Δf = 20 kHz, f_o = 45 MHz, λ = 830 nm

21. Variation of signal ratio Sn/So with nearest neighbour pixel number for the case of Δf = 10 MHz, f_o = 1 GHz, λ = 830 nm

22. Scheme for chromatic compensation of Bragg cell spectrum analyser

1. INTRODUCTION

Acousto-optic Bragg cell processors are currently being considered as possible candidates for the next generation of ESM receivers. AO processors have potential for surveillance and warning applications in both radar and communication frequency bands. They have the potential to provide wide bandwidth coverage in real time with high probability of intercept. Bragg cells with bandwidths of 1 GHz centred on 3 GHz are currently available and bandwidths of 2 GHz centred on 4 GHz and with a deflection efficiency of 5%/W are projected in the near future. The frequency band from 2 to 18 GHz could thus be covered by eight parallel channels and suitable mixing arrangements. At communication frequencies, bandwidths of 50 MHz are currently available with adequate (20 kHz) resolution and deflection efficiencies of order 100%/W. AO processors also have the significant advantage of a simultaneous frequency/direction of arrival measurement capability using suitable interferometric architectures. This additional capability is considered highly desirable as a powerful aid in sorting signals in a complex environment eg, an environment containing several frequency hopper sources.

Most laboratory development of AO processors is carried out using a gas laser, usually Helium-Neon, as the light source. Any practical receiver to be used in the field, for reasons of weight, size, cost and robustness will preferably use a laser diode as the optical source. It has recently been recognised however that the spatial and spectral characteristics of the laser diode may result in a degradation in the performance of the spectrum analyser. Workers at the US Naval Research Laboratory have considered some aspects of these effects(ref.1), looking particularly at the effect of spectral width on integrated optic AO processors operating at radar frequencies. In this paper the effect of both the spatial and spectral characteristics of laser diodes on AO processors operating at the communication frequencies will be examined and it will be shown that the effects are considerably more severe at these lower frequencies. Some techniques for reducing the resulting performance degration will be discussed. As a preliminary to this consideration, the basic structure and characteristics of semi-conductor laser diodes will be reviewed in the next section, with emphasis on those properties affecting their performance in AO spectrum analysers.

2. LASER DIODE SOURCES

2.1 Introduction

Semi-conductor lasers, as opposed to Helium-Neon lasers, are still an immature technology but also one in which rapid strides are being made, being driven largely by the requirements of optical fibre communications. Laser diodes are semi-conductor diodes, typically made of Gallium Arsenide and Aluminium Gallium Arsenide crystals for radiation in the near infrared. Radiation is emitted by recombination at a wavelength proportional to the band energy gap in the laser active region. In order for lasing to take place a sufficiently high concentration of carriers must be injected into the active region to induce population inversion. This may be accomplished using a double hetero-junction structure (see figure 1) as is used in the Hitachi Series 1000 laser diodes(ref.2). The thin active layer of n-type $Al_x Ga_{1-x} AS$ is sandwiched between n and p-type $Al_y Ga_{1-y} AS$ layers ($x < y$) which have wider band gaps and lower refractive indices than the active layer. Here x and y are the mole fractions of Al in the Al Ga alloy. Electrons and holes injected into the active region through the hetero-junction are accumulated because of the potential barriers at the hetero-boundaries. The active layer thickness is typically 0.1 μm and this forms

an efficient optical waveguide because of the refractive index difference between the active and sandwiching layers. Optical feedback is provided by a pair of mirror facets at each end of the device. These are usually formed simply by cleaving the crystal along a crystal plane effectively forming a Fabry-Perot cavity.

2.2 Single mode lasers

Laser diodes suitable for use in AO processors must be of the single mode variety to ensure a narrow, well shaped beam. Both transverse and longitudinal laser oscillation modes are possible in the active junction and a single mode laser is one which oscillates in the fundamental transverse mode only (transverse and longitudinal here refer to direction with respect to the junction). This can be accomplished by controlling the crystal growth so that a waveguide is created which confines the active region into a narrow horizontal strip, sufficiently narrow that no higher-order horizontal modes can propagate. Various index-guiding architectures have been developed, examples are:

CDH - constricted double heterostructure device, which uses laternal variations in the active layer thickness above a mesa etched into the substrate to contain the lasing region(ref.4).

CHD-LOC - large optical cavity, a passive waveguide layer is added to the active CDH layer which reduces the optical density and thus the chance of damage to the exit facets without generating multiple lateral modes(ref.5).

BH - buried heterostructure devices, in which the active region is completely surrounded by low refractive index material(ref.6).

These index guiding structures generally result in a narrow radiated beam that is approximately Gaussian but with significant deviations which will be discussed later. Typical emission full width angles are 30° perpendicular to the junction and 10° parallel to the junction.

2.3 Single frequency lasers

Single transverse mode lasers may however operate in a range of longitudinal modes producing an output spectrum such as that shown in figure 2(a). Each line corresponds to a longitudinal propagation mode and their separation will depend upon the cavity length. For use in an AO processor a source which is spectrally pure is highly desirable to ensure no degradation of resolution or dynamic range. To complicate matters further, the number of modes excited depends strongly on the drive current. A variety of diode architectures are currently being considered which will reinforce one longitudinal mode and suppress all unwanted modes, thus forcing a single frequency laser. A description of a number of these experimental devices may be found in reference 3. These may be summarised in four main types:

(i) Coupled-cavity lasers: an additional external cavity is included through which the laser light passes, re-inforcing only the wavelength which resonates in both the external and internal cavity eg an external mirror, parallel to the end mirror of the laser, see figure 3(a). Note: difficult to tune.

(ii) Frequency-selective feedback laser: inclusion of an external cavity which contains a frequency selective element, eg a diffraction grating, which allows tuning by tilting the grating; see figure 3(b).

(iii) Injection locked laser: forces diode to operate at a single wavelength by using a single wavelength source as an external driver; see figure 3(c).

(iv) Geometry controlled laser: principal example is the short cavity laser in which the cavity is only about 50 μm long. The short length forces the unwanted modes to be widely separated in wavelength from the wanted mode, and by including highly reflective coatings on the facet mirrors an essentially single frequency laser can be achieved; see figure 3(d).

Many variations on these architectures have been proposed. Figueroa et al(ref.7) describe the use of an optical fibre external resonator with a lens formed at the fibre tip to provide beam refocussing into the active region of the laser. Vanderleeden(ref.8) describes a frequency selective feedback laser which uses a guided index fibre lens to form an optically dispersive cavity, see figure 4. A diffraction grating is deposited on the other end of the fibre. By varying the position of the laser in the x-direction as indicated, the angle of incidence on the grating and thus the frequency reinforced can be varied. This provides an effective means of tuning the resulting single frequency laser. This approach is very promising and may lead to the development of useful single frequency lasers.

However, none of these proposed techniques has yet reached commercial production, the optimum spectrally pure lasers currently available being single mode lasers with index guiding as described above. These structures have the significant advantage that between certain drive current limits they tend to radiate at a single longitudinal mode. Thus provided the current is above a certain threshold and below a given maximum a single stimulated frequency of emission is achieved. Typically, for the Hitachi Laser Diode 1000 series, the suppression ratio of the unwanted longitudinal modes is approximately 29 dB, the modes being separated in wavelength by approximately 0.3 nm(ref.2).

It is worth noting that the obvious solution of using a narrow bandwidth multi-layer bandpass filter to select a single frequency fails, even if such a high performance device could be designed and fabricated, because of the phenomena known as partition noise. A laser resonating at several longitudinal modes acts as a coupled oscillator, the total energy remains the same but the share of any particular mode varies with time. Thus if one mode could be filtered out, unacceptable fluctuations in the amplitude of the laser would occur.

2.4 Spontaneous emission

Accompanying the stimulated emission in any laser diode is a level of broadband incoherent spontaneous emission which will produce spurious detector outputs in an AO spectrum analyser and thus degrade its performance. An example of spontaneous emission surrounding the single laser line for a General Optronics Laser diode is shown in figure 5 obtained from reference 1. The spectrum was measured using a spectrometer with a bandpass of approximately 0.1 nm. The spectrum is approximately 6 nm wide at three orders of magnitude down from the peak and 20 nm wide at five orders down. The emissions contain both TE and TM polarisations in contrast to the narrow band TE stimulated emission laser output(ref.9).

Streifer et al(ref.9) have been particularly successful in reducing the emission levels by increasing the rear facet reflectivity and by the use of a spatial filter on the front facet which absorbs much of the spontaneous emission but which transmits most of the stimulated radiation. A Te mask is deposited on the front facet and an aperture oblated by the laser itself which is then stabilised by a further coating. Te is highly absorptive at the wavelength of interest. The data shown in figure 5 was for a laser which had been treated in this way. As outlined in Section 1, the effect of the presence of this level of spontaneous emission on the AO spectrum analyser will be considered in following sections.

2.5 Data availability and operational considerations

The most important characteristics of laser diodes determining their suitability for use in AO spectrum analysers are:

(i) spectral purity

(ii) optical beam shape

(iii) robustness of operation.

A number of approximately single frequency laser diodes with index guiding are currently available commercially, the best performing being the Hitachi HLP-1000 series of diodes and the General Optronics GOLS-4000 and 5000 diodes. However very little published data is available showing results of measurements of intensity versus frequency over more than one or two orders of magnitude. Reference 1 provides the only detailed spectral measurements for several General Optronic models with Te masks and for the HLP-1400 diode. A full emission spectral profile is given only for one of the General Optronic diodes, as shown in figure 5, and these measurements will be used in this paper to assess the expected effects on AO spectrum analyser performance. Clearly further detailed spectral measurements of candidate laser diode sources are required.

The shape of the optical beam effectively determines the aperture weighting function for the Bragg cell in an AO spectrum analyser (see fuller discussion in Section 3) which in turn determines the resolution and side-lobe levels. Again very little published data is available beyond manufacturers' data showing beam profiles over one order of magnitude. The Application Manual for the Hitachi HLP-1000 Series(ref.2) provides typical far-field patterns (see figure 6) for this range of diodes covering about one order of magnitude and for several output power levels. These show that the profiles are approximately Gaussian in shape and are markedly different for directions perpendicular and parallel to the laser junction. The beam parallel to the junction is narrower and a closer approximation to a Gaussian. Profiles report in references 5, 6, 10 and 11 for various laser diodes structures show a range of profiles, some of which differ markedly from Gaussian. Again, further detailed measurements of candidate laser diodes profiles are required. In this paper the effects of various hypothetical profiles will be investigated to obtain an estimate of the importance of this characteristic.

In considering the use of laser diode sources in AO systems a number of operational factors must also be considered. Considerable care must be taken to ensure stable operation for a laser diode as the power versus current curve is steep and temperature sensitive. Typical curves for the Hitachi HLP-1000 series are shown in figure 7. The longitudinal oscillation mode frequency is also temperature and current dependent since the refractive index of the active layer which determines the lasing

frequency is itself dependent on these two variables. The lasing wavelength may change by about 0.3 nm/°C so that the drive current and the temperature must be highly stabilised using a Peltier cooling device and associated feedback circuitry.

A promising new development in this area was reported recently by Bowers et al(ref.12). The authors here fabricated a cleaved-coupled-cavity laser (C^3) with a large cavity length ratio which allows an enhanced stability performance. The C^3 laser, a version of the single frequency coupled cavity type outlined above, consists of a normal single mode laser diode which is broken into two unequal sections by cleaving along a crystal face. The shorter cavity is used as the frequency modulator and the combination of short and long cavities has a much greater frequency stability against temperature and injection current changes. The dominant lasing mode dependence on temperature and current measured in reference 12 is shown in figure 8. The mode hop boundaries are shown by solid lines and the greater than 100:1 peak to sidelobe region is indicated by a dashed line. Useful stable single frequency operation has been achieved over a wide range of current and temperature values.

The laser is also extremely sensitive to small amounts of its own light that may be reflected back into the lasing cavity(ref.13). It is also fragile and susceptible to damage from supply spikes and electrostatic discharges. Other factors which must be considered if the laser is to be modulated for use in for example, an AO correlator, are linearity and frequency response. As can be seen from figure 7, for linear analogue operation the laser must be operated above the threshold current necessitating a continuous bias current. Finally it should be noted that semi-conductor lasers experience a slow degradation in their characteristics as the number of working hours increases and their performance must be monitored at regular intervals to ensure correct operation. Performance in this regard is improving continuously through new research.

Despite these current operational problems it is expected that semi-conductor lasers will improve in performance and will be used in a variety of AO processors due to their obvious size and cost benefits and also to their modulation capabilities.

3. AO SPECTRUM ANALYSER

3.1 Basic analyser

The basic structure of an AO spectrum analyser is illustrated in figure 9. The Bragg cell converts the input electrical signal f(t) into a travelling optical index modulation across the cell aperture. This modulation is impressed on the collimated input laser beam to form an optical analogue of the electrical input. A lens produces the Fourier transform of the weighted signal as it forms the far field diffraction patterns in its back focal plane. This transform is detected by a photodiode array in the frequency plane, the elements of which respond to optical intensity. The intensity distribution in the frequency plane is thus proportional to the power spectrum of the input signal.

The frequency spectrum so measured is approximately linear in the frequency scale (small angle approximation) and is linear in intensity to limits set by acousto-optic non-linearities and non-linearities in input electronics and the detector array.

Design considerations for AO Bragg cells are discussed in detail in reference 14. For a deflector cell, the key performance parameters are the bandwidth B, the aperture τ, the diffraction efficiency I_1/I_0 (the percentage of incident light diffracted into the first order beam for incidence at the Bragg angle), the acoustic attenuation in the cell, and the number of resolvable spots or frequencies in the frequency plane, N, the upper limit of which is given by

$$N = B\tau. \tag{1}$$

The spectrum analyser weighting function is determined by the input laser beam amplitude profile after limitation by the finite cell aperture and the acoustic attenuation in the cell(ref.15). These weighting functions may be expressed in terms of time variables as follows. The finite aperture size, D, of the Bragg cell imposes a unity amplitude window function

$$W_1(t, \tau) = \text{rect}(t/\tau - 1/2) \tag{2}$$

where $\tau = D/v_a$ and v_a is the acoustic velocity in the cell.

The acoustic wave in the cell is attenuated as it propagates which effectively modifies the impressed modulation by the weighting function W_2, where

$$W_2(t, \alpha, \tau) = \exp(-\alpha t) \tag{3}$$

α is the frequency dependent loss factor given by

$$\alpha = \Gamma f^2 V_a/20 \log_{10}\ell \tag{4}$$

and Γ is the material acoustic loss coefficient ($dB/cm/GHz^2$).

The third weighting function is the optical beam amplitude profile. Gas lasers usually have an approximately Gaussian beam amplitude cross-section of the form

$$W_3(t, \tau, T) = \exp[-4T^2(t/\tau - 1/2)^2] \tag{5}$$

where $T = D/2w_o$, the ratio of the Bragg cell aperture to the Gaussian beam waist at the $1/e^2$ intensity level. The Gaussian weighting is very useful in that it results in suppression of the sidelobes for a small sacrifice in resolution.

The overall weight factor is thus a product of three individually weights W_{1-3} with W_3 chosen appropriately. Hecht(ref.15) has investigated the effects on resolution and sidelobes of various Gaussian profiles using simplifying assumptions which allow the Fourier integral equations to be solved. Here the spectrum analyser performance is modelled on the computer

using the Fast Fourier Transform to evaluate the Discrete Fourier Transform which allows a study of the effects of various beam profiles.

3.2 Computer model

The computer model developed is for a spectrum analyser operating at communication frequencies using an Isomet Corporation Bragg cell Model OPT-1. This is a Tellurium Dioxide cell with the following properties:

Bandwidth	:	30 MHz
Centre Frequency	:	45 MHz
Aperture (τ)	:	50 μs
Bτ Product	:	1500
Acoustic Velocity	:	616 m/s (shear mode)
Acoustic Loss coefficient (Γ)	:	290 dB/cm/GHz^2

The maximum number of resolvable spots in the frequency plane is thus 1500, corresponding to a frequency resolution of 20 kHz. The AO spectrum analyser performance is modelled by the following calculations:

(i) generating a 50 μs sample of the signal to be processed, sampled at a rate commensurate with the Nyquist criteria,

(ii) filling out this sample to 200 μs with zeros to provide a 5 kHz resolution in the FFT,

(iii) applying appropriate aperture weighting factors in the time domain,

(iv) calculating the Fast Fourier Transform of this series,

(v) applying appropriate weighting factors in the frequency domain,

(vi) averaging the estimates over a linear distance in the frequency plane corresponding to a pixel width, and

(vii) plotting the resultant power frequency spectrum.

The weighting factors in the frequency domain may be included to account for the pass-band shape of the Bragg cell which will depend upon the pass-band shape of the transducer and the variation in diffraction efficiency of the acousto-optic interaction with frequency. Theoretical expressions for these factors are given in references 14 and 15 for normal and bi-refringent cells, the latter case applying to the OPT-1 cell being used here. Alternatively the measured deflection efficiency versus frequency curves provided by the manufacturer can be used. In the results reported here, these factors are held at unity as their effects are not important for the purposes of the study.

The results for a CW signal of frequency 45 MHz are shown in figure 10. Figure 10(a) shows the power spectrum obtained without pixel averaging (steps (vi) above) illustrating the sidelobe structure corresponding to the aperture width of 50 μs. The time bandwidth product of the Bragg cell is 1500, corresponding to a frequency resolution 20 kHz. The optics of a

spectrum analyser would thus be adjusted so that each pixel in the output photodiode array covered a distance in the frequency plane corresponding to this resolution. Step (vi) above is therefore included to take account of this averaging of the spectrum over each pixel and the resultant power spectrum for the 45 MHz CW signal is shown in figure 10(b). The sidelobe structure resulting from the finite cell aperture has been smoothed out by this averaging process. However significant power has spilled over into adjacent frequency bins from the "wanted" signal at 45 MHz which will limit the ability to detect the presence of other signals close in frequency. A commonly used parameter to measure this effect is the "adjacent frequency dynamic range", which in this case has been reduced to 22 dB.

Signals with duration shorter than 50 μs will produce significant lobe structures which will seriously reduce the performance of the spectrum analyser. An example shown in figure 11 is for a 10 μs burst of CW at 45 MHz. Adjacent frequency dynamic range has been reduced to less than 2 dB and the lobe structure would effect measurements many pixels away from the "wanted" peak at 45 MHz. Clearly a centroiding procedure would be required to allow the wanted frequency to be selected and prevent multiple signal reports in the ESM receiver, however the dynamic range performance for the detection of nearby frequencies would still be severely limited. In figure 11 the 10 μs signal has been assumed to be fully in the cell aperture. A broader, varying sidelobe structure would be observed as the signal enters and leaves the cell.

In the next Section the procedure described here for studying the spectrum analyser performance will be used to study the effect of varying laser beam profiles.

4. LASER BEAM PROFILE

4.1 Effect of Gaussian beam shape

Gas lasers and to a lesser extent, semi-conductor lasers, have a far field beam amplitude profile which approximates the Gaussian form given in equation (5) above. Light intensity profiles are shown in figure 12 for various values of the parameter T, the ratio of the Bragg cell aperture to the Gaussian beam waist at $1/e^2$ intensity level. The effect of a Gaussian profile on the AO spectrum analyser performance is shown in figure 13 for various values of T for the case of a CW signal of 45 MHz. As T is increased from zero, corresponding to a flat weighting, the sidelobe level at pixels well removed from the wanted pixel is seen to be reduced significantly, resulting in an increased available dynamic range. However this reduction is achieved at the expense of a broadening in the main lobe, reducing the resolution and the available dynamic range in the near pixels. These effects are summarised in figure 14 and 15. In figure 14 the beam spread factor (the resolution change in the 3 dB beamwidth) is plotted as a function of T. In figure 15 the available dynamic range is plotted as a function of T for various pixel separations from the "wanted" pixel.

The choice of an optimum value for T will be a compromise which will depend heavily on the dynamic range required. The maximum dynamic range in AO receivers is limited principally by the dynamic range of the photodetectors. The best dynamic range available in current photodiode arrays is approximately 40 dB, whereas discrete diodes eg avalanche photodiodes, can achieve approximately 80 dB. In applications such as radar warning receivers where only a fairly coarse resolution is required eg 10 MHz in a bandwidth of a 1 GHz, then discrete photodiodes can be used as only a relatively small number are required.

For this case a larger value of T can be chosen to give the required sidelobe suppression. For application in the communication frequency bands, high resolution is required over a wide bandwidth, typically 25 kHz resolution over 30 MHz or more, so that a photodiode array must be used with the corresponding dynamic range limitation. Thus from figure 14 and 15 a choice of T in the range 1.5 to 2 would provide the full photodiode array dynamic range of 40 dB for all pixels beyond the second pixel from the wanted frequency with a beam spread ratio of approximately 2.

The use of Gaussian weighting of the laser beam profile implies an overall intensity loss compared with uniform aperture weighting as the full aperture is not being utilised. This loss is shown as a function of T in figure 16. This loss has not been included in the calculations for figures 13 to 15 as it has been assumed that sufficient light intensity is available to fully utilise the photo-detector dynamic range.

It should be noted that in this report the effect of the use of a laser diode in an AO receiver is being considered. Many other factors come into the overall receiver design including noise considerations, ripple factor (response to CW signals midway between adjacent channels), optical and electrical crosstalk between channels in the photodiode array and in the readout process and dynamic range limitation due to light scatter, photodetector dark currents and two tone third order intermodulation products.

4.2 Laser diode beam profiles

Far field beam profiles for double hetero-junction diode lasers have been studied theoretically by several workers. Botez and Ettenberg(ref.16) derive theoretical expressions for the beamwidth from a study of the electric fields in the active region of the diode and show that these can be approximated by a Gaussian beam if the parameter

$$R = (2\pi\, d/\lambda)\ (n_1^2 - n_2^2) \qquad (6)$$

lies in the range $1.5 < R < 6$, where d is the active layer thickness, λ the laser wavelength and n_1 and n_2 are the refractive indices of the active and sandwiching layers respectively. For values of $R < 1.5$ the Gaussian beamwidth approximation is no longer appropriate. The near field patterns have double exponential shapes and become relatively wide, which in turn gives far field patterns of narrow beamwidth and non-Gaussian shapes. For $R < 1.5$, a Gaussian severely underestimates the far field pattern at intensity below the -3 dB level(ref.16).

Reference 2 provides details of the parameters of the Hitachi HLP-1000 series of double-heterojunction diodes, which allow R in equation (6) to be evaluated. These are: $n_2 \approx 3.6$, $d = 0.1$ µm, $\Delta n = 0.05$, $\lambda = 830$ nm. A value of $R \approx 0.35$ results, indicating that these diodes might be expected to exhibit far field beam profiles significantly different from Gaussian. This conclusion is borne out by the manufacturers typical profiles for this diode shown in figure 6. The profile shape diverges from Gaussian below the $1/e^2$ intensity level. Discussions with US Naval Research Laboratory personnel indicate that laser diode beam profiles also frequently exhibit sharp discontinuities or "glitches" in intensity level with direction. In order to obtain an order of magnitude estimate of the effects of these variations from pure Gaussian on the spectrum analyser performance, model

calculations were made with the weighting profiles shown in figure 17. Curve A is the pure Gaussian intensity profile, curve B represents the case where the profile flattens out at the $1/e^2$ intensity level and curve C represents a "glitch" in the profile occuring at the $1/e^2$ level in which the amplitude reduces by a factor of 0.5.

The effects of these variations from Gaussian will depend upon the value of the parameter T selected, clearly for T less than unity no effect would be observed. Model results for the case of T = 2.2 are shown in figure 18. The deviations from Gaussian produce significant increases in sidelobe levels for both intensity curves B and C of figure 17, the levels being increased by +24 dB and +31 dB respectively at pixels removed from the "wanted" pixel. Further model results are set out in Table 1. The dynamic range and resolution performance of the AO spectrum analyser will clearly be strongly effected by the goodness of fit of the laser beam profile to a Gaussian profile. Laser diode sources to be used in AO receivers must clearly be carefully selected on their beam profile characteristics which must be known down to 3 to 4 orders of magnitude below the peak level, depending upon the choice of the truncation parameter T. Consideration may also need to be given to shaping the laser profile to more closely approximate a Gaussian. One possibility is to use a layer of absorbent material of varying thickness as shown in figure 19. Materials such as Schott-filter glass could be used to construct such an element. Alternatively a graded film mask could be used.

5. LASER EMISSION SPECTRUM

5.1 Effect on spectrum analyser performance

Few detailed measurements of laser diode emission spectra are available in the literature. One of the measurements available is the spectrum for the General Optronics Model GOLS-1/TB47 as shown in figure 5 (from reference 1). This diode has been especially fabricated using a Tellurium mask to reduce spontaneous emission levels as discussed in Section 2.4 above. The measurements were made with a spectrometer of bandpass $\Delta\lambda_s$ = 0.1 nm. The measured signal can be written as

$$S(\lambda) = T P_\lambda \Delta\lambda_s \tag{7}$$

where T is the spectrometer transmission and P_λ the laser spectral power. Assuming the laser spectral peak to be very narrow in bandwidth compared to the spectrometer bandpass so that at the peak an intensity proportional to the total laser power P_o is measured, then

$$S_{peak} = TP_o \tag{8}$$

In figure 5, $R(\lambda)$ is plotted, where

$$R(\lambda) = S(\lambda)/S_{peak} \tag{9}$$

Thus the spectral power is obtained from

$$P_\lambda = R(\lambda)\, P_o/\Delta\lambda_s \tag{10}$$

For an AO spectrum analyser operating in the Bragg regime the optical deflection angle θ is given by

$$\theta = \lambda_o f/nv_a \tag{11}$$

where n is the optical refractive index of the Bragg cell material and V_a is the velocity of bulk acoustic wave. If the frequency resolution of the spectrum analyser Δf corresponds to a single pixel in the detector array for a monochromatic source of wavelength λ_o, then the optical pixel width $\Delta\lambda_p$ is given by

$$\Delta\lambda_p = \lambda_o \Delta f/f \tag{12}$$

The optical power at the wanted pixel will be P_o and the power at the nth nearest neighbouring pixel will then be $P_\lambda(\lambda_n)\,\Delta\lambda_p$. The ratio of the signal in the nth nearest pixel S_n to the signal in the wanted pixel S_o is given by

$$S_n/S_o = P_\lambda(\lambda_n)\,\Delta\lambda_p/P_o \tag{13(a)}$$

$$= R(\lambda_n)\,\Delta\lambda_p/\Delta\lambda_s \tag{13(b)}$$

where λ_n denotes the wavelength at the nth pixel. The ratio in equation (13(b)) may be considered as normalising the measured relative intensity from the spectrometer resolution $\Delta\lambda_s$ to the spectrum analyser resolution $\Delta\lambda_p$. Using the measured data for the General Optronics diode show in figure 5, the ratio S_n/S_o was calculated for the spectrum analyser with the following characteristics: f = 45 MHz, Δf = 20 kHz, λ_o = 830 nm. The results are shown in figure 20 plotted against pixel member. Also shown is the spectrum analyser performance for a monochromatic source and a Gaussian profile (T = 2.2) taken from figure 18. The available dynamic range for adjacent pixels and the resolution will clearly be dominated by the energy spread due to the laser diode spectral content. A full dynamic range of 40 dB is only available beyond approximately ±20 pixels from the wanted pixel ie a frequency range of ±400 kHz. This would impose a serious limitation on the AO spectrum analyser performance and a laser diode with very much improved spectral characteristics would be required. The effect on spectrum analyser performance is considerably worse for the high resolution case at communication frequencies shown in figure 20 than for the radar case. For example, the case of a spectrum analyser with characteristics typical for radar warning receiver applications is shown in figure 21. Here the bandwidth is 1 GHz and the resolution 10 MHz. The overall signal levels in the adjacent pixels are higher but the number of pixels effected is very much reduced due to a change in the value of $\Delta\lambda_p$. The effect would be considerably more serious however if a dynamic range of 80 dB was sought for this case.

It should be noted that the ratio $\Delta\lambda_p/\Delta\lambda_s$ in equation (13(b)) can lie in the range 1 to 100 for cases of interest so that the intensity ratio $R(\lambda)$ must be measured over up to two orders of magnitude more than the performance dynamic range required.

5.2 Improved emission spectrum

5.2.1 Use of filter

The most obvious method for reducing the effects of spontaneous emission spectrum on the AO spectrum analyser performance is the use of a very narrow bandwidth multi-layer passband filter. As mentioned earlier, a filter cannot be used where feedback to the laser diode can occur as this simply shifts the lasing wavelength to the point of maximum reflectivity. However a filter could be used provided it was isolated from the laser source. A typical two cavity design operating at normal incidence would have a half power bandwidth of 2.6 nm and a 1/10 power bandwidth of 5 nm. This filter would have a useful effect on the spectrum of figure 5, providing a full 40 dB dynamic range for pixels beyond about ±12 for the case of the high resolution spectrum analyser of figure 20. A sharper passband shape would be required to fully overcome the wide spectrum bandwidth problem. Off-normal incidence multi-layered filters could be considered although polarisation effects may be a problem. The recent development of LYOT filters fabricated using optically active substrates also holds promise for very narrow band filters(ref.16).

5.2.2 Chromatic compensation

An alternative method for overcoming the broad spectrum problem is to use some form of chromatic compensation. In the acoustic-optic interaction, the optical diffraction angle θ' is related to the incident angle θ by (ignoring material effects)

$$\theta' = \lambda_o/\Gamma - \theta$$

where λ_o is the optical wavelength and Γ the acoustic wavelength. If $\theta = \theta_{B_o} = \lambda_o/2\Gamma$, the Bragg angle, then $\theta' = \theta_{B_o}$ which is the condition for most efficient diffraction. If light of wavelength λ_1, enters at $\theta = \theta_{B_o}$, then

$$\theta' = \lambda_1/\Gamma - \lambda_o/2\Gamma$$

$$= \theta_{B_o} + \Delta\lambda/\Gamma \qquad (15)$$

where $\Delta\lambda = (\lambda_1 - \lambda_o)$. The second term in equation (15) represents the undesired error in the diffracted angle which causes the spread of energy in the detector plane. One method of compensating for this change in wavelength would be to include an element which produces an incident angle to the Bragg cell which corrects the error in equation (15) with frequency. This could be simply achieved with a diffraction grating as shown in figure 22. The condition for a diffraction maximum in the grating for oblique incidence is given by

$$d(\text{Sin}\ \theta'_G - \text{Sin}\ \theta_g) = p\lambda \quad |p| = 1,2,3.. \qquad (16)$$

where d is the grating spacing and θ_G and θ'_G the incident and diffraction angles.

For the first maximum (p = 1) and assuming θ_G small,

$$d(\theta'_G - \theta_g) = \lambda$$

Thus if d = Γ, the acoustic wavelength in the Bragg cell and $\theta_G = \theta_{B_o}$, then

$$\theta'_G = \theta_{B_o} + \lambda_o/\Gamma$$

for $\lambda = \lambda_o$ and

$$\theta'_G = \theta_{B_o} + \lambda_1/\Gamma$$

$$= \theta_{B_o} + \lambda_o/\Gamma + \Delta\lambda/\Gamma$$

for $\lambda = \lambda_1$. θ'_G now becomes the incident angle for the Bragg cell and will give rise to the correction term required in equation (15) to ensure a final diffracted angle independent of optical wavelength. Diffraction gratings with the necessary line spacing should be readily realisable and the proposed method of chromatic compensation holds promise for correcting the wide frequency content of the laser diode source.

6. SUMMARY

In this paper the effect of using a laser diode as the light source for an acousto-optic spectrum analyser has been examined. The particular laser diode characteristics which limit the performance of the spectrum analyser are the laser beam profile shape and the laser power spectrum. The effect of these characteristics has been studied using a computer model of an AO spectrum analyser which models the analyser performance using the Fast Fourier Transform. The particular spectrum analyser studied has been a high resolution processor appropriate for communication frequencies with a bandwidth of 30 MHz and resolution 20 kHz.

Gaussian weighting of the laser beam intensity profile has the desirable effect of reducing sidelobes. However it has been shown that variations from a Gaussian beam which might be expected to occur in laser diodes can cause serious increases in sidelobe levels and thus major reduction in dynamic range performance. Careful measurement of the laser beam profile shape will be required before use in an AO spectrum analyser, and the depth of measurement required will be a function of the Gaussian truncation selected. Consideration may have to be given to beam apodisation using variable thickness absorbing materials.

Laser spontaneous emission occuring over a wide range of wavelengths surrounding the lasing wavelength in a single frequency laser can cause serious reduction in the AO spectrum analyser performance. For the high resolution analyser available dynamic range was severely limited out to ±20 pixels from the wanted pixel for the laser diode emission profile studied. The effect is not as serious for high-frequency, lower-resolution analysers. To predict the suitability of a particular laser diode the emission intensity profile must be measured out to several orders of magnitude greater than the dynamic range desired.

Methods for reducing the effect of the broad spectral content of the laser diode have been considered and a technique for chromatic compensation proposed which holds promise for markedly improved performance. The next generation of single frequency laser diodes currently under development also holds promise of improved performance.

A marked lack of complete data on laser beam profiles and emission spectra was noted both in the literature and in manufacturer's data.

TABLE 1. INCREASE IN SIDELOBE LEVEL AT PIXELS DISTANT FROM WANTED PIXEL DUE TO NON-GAUSSIAN BEAM PROFILE

	T = 1.5	T = 2.2
Glitch -0.5	+3 dB	+24 dB
-0.1	+8 dB	+30 dB
Flat ($1/e^2$)	+11 dB	+31 dB

REFERENCES

No.	Author	Title
1	Burns, W.K. and Moeller, R.P.	"Effect of Laser Diode Spontaneous Emission on IOSA Operation". Applied Optics 20, 913, 1981
2	-	"Hitachi Laser Diode: Applications Manual".
3	Bell, T.E.	"Single Frequency Semi-Conductor Lasers". IEEE Spectrum December 1983
4	Botez, D.	"Applied Physics Letters 33, 872, 1978".
5	Botez, D.	"CW High Power Single Mode Operation of CDM Al Ga As Lasers with Large Optical Cavity". Applied Physics Letters 36, 190, 1980
6	Chinone, N., Saito, K., Ito, R. and Aiki, K.	"Highly Efficient GaAlAs Buried Heterostructure Lasers with Buried Optical Guide". Applied Physics Letters 35, 513, 1979
7	Figueroa, L., Lau, K.Y., Yen, H.W. and Yariv, A.	"Studies of GaAlAs Injection Lasers Operating with an Optical Fiber Resonator". J. Applied Physics 51, 3062, 1980
8	Vanderleeden, J.C.	"A Proposal for Wavelength Tuning and Stabilisation of GaAs Lasers with a Graded Index Fibre Segment in a Dispersive Cavity". Optoelectronics 6, 443, 1974
9	Streifer, W., Ponce, F.A. and Scrifes, D.R.	"Reduction of GaAs Diode Laser Spontaneous Emission". Applied Physics Letters 37, 10, 1980
10	Botez, D. and Connolly, J.C.	"Terraced Heterostructure LOC AlGaAs Diode Laser: A New Type of High-power CW Single Mode Device". Applied Physics Letters 41, 310, 1982
11	Itek Corporation	"Angle of Arrival Sensors Using Acousto-Optical Processing". Report No. N00173-76-C-0333, March 1977
12	Bowers, J.E., Bjorkholm, C.A., Burrus, C.A., Coldren, L.A., Heneway, B.R. and Wilt, D.P.	"Wave-coupled-cavity Lasers with Large Cavity Length Ratios for Enhanced Stability". Applied Physics Letters 44, 821, 1984

No.	Author	Title
13	Fujiwara, M., Kuboth, K. and Lang, R.	"Low Frequency Intensity Fluctuations in Laser Diodes with External Optical Feedback". Applied Physics Letters 38, 217, 1981
14	Young, E.H. and Yao, S.K.	"Design Considerations for Acousto-optic Devices". Proc. IEEE 69, 54, 1981
15	Hecht, D.L.	"Spectrum Analysis Using Acousto-Optic Devices". Optical Eng. 16, 461, 1977
16	Venning, J.	Personal Communication

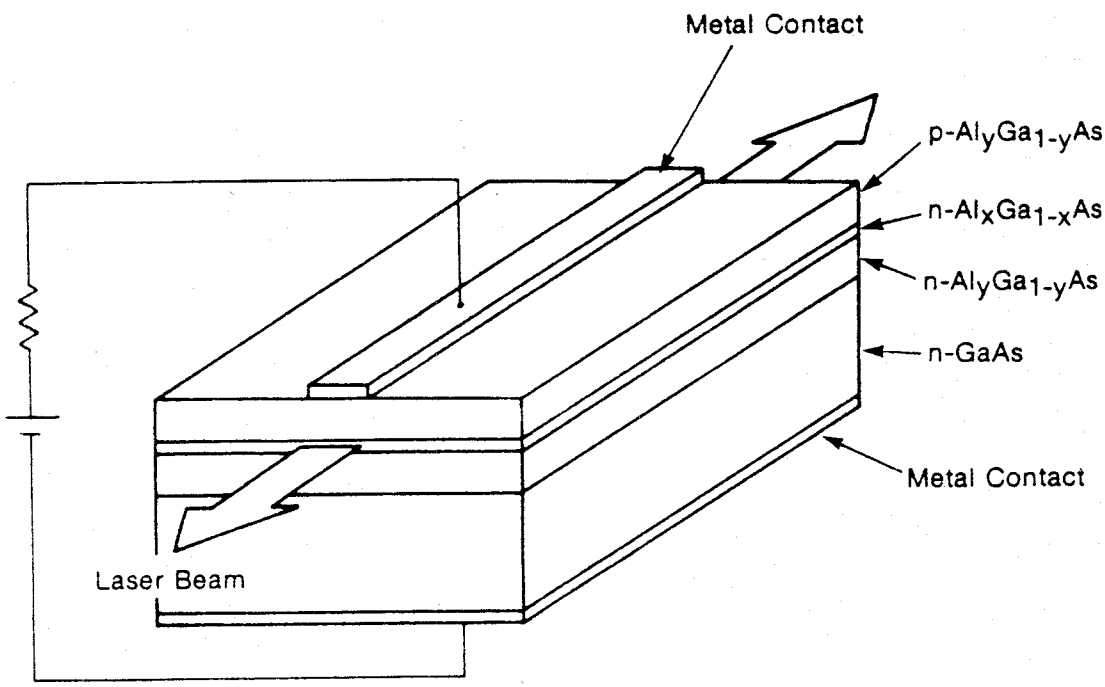

Figure 1. Double hetero-junction laser diode construction (from reference 2)

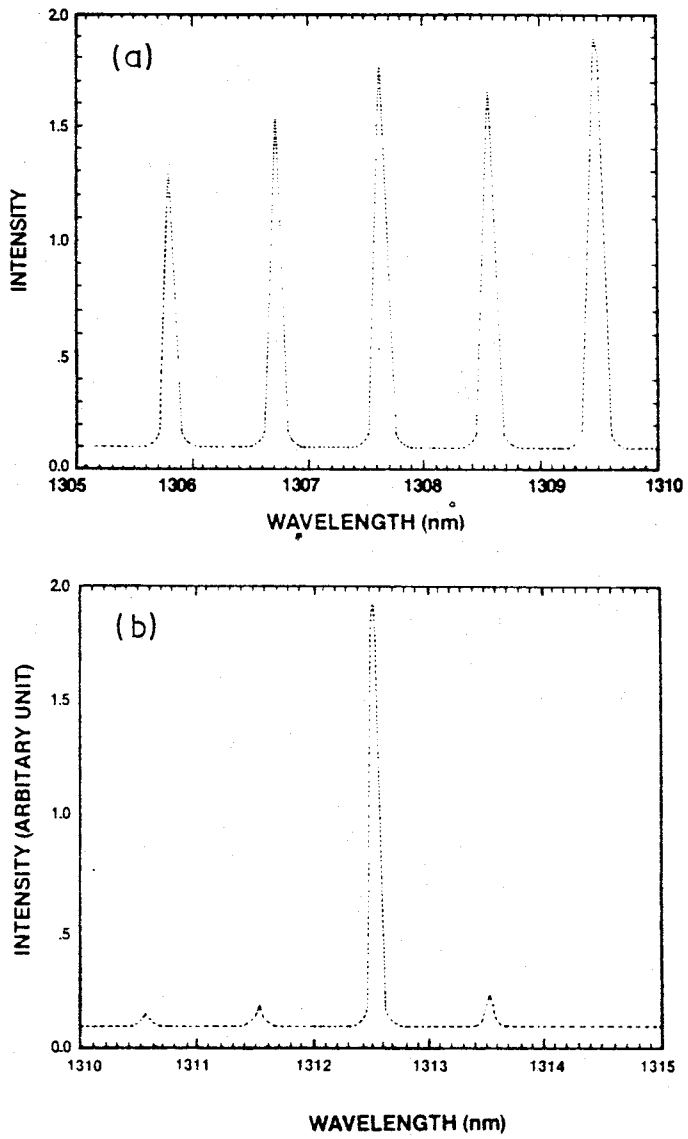

(a) Output spectrum of multi-longitudinal mode laser

(b) Output spectrum of single frequency laser

Figure 2. Laser output spectrum

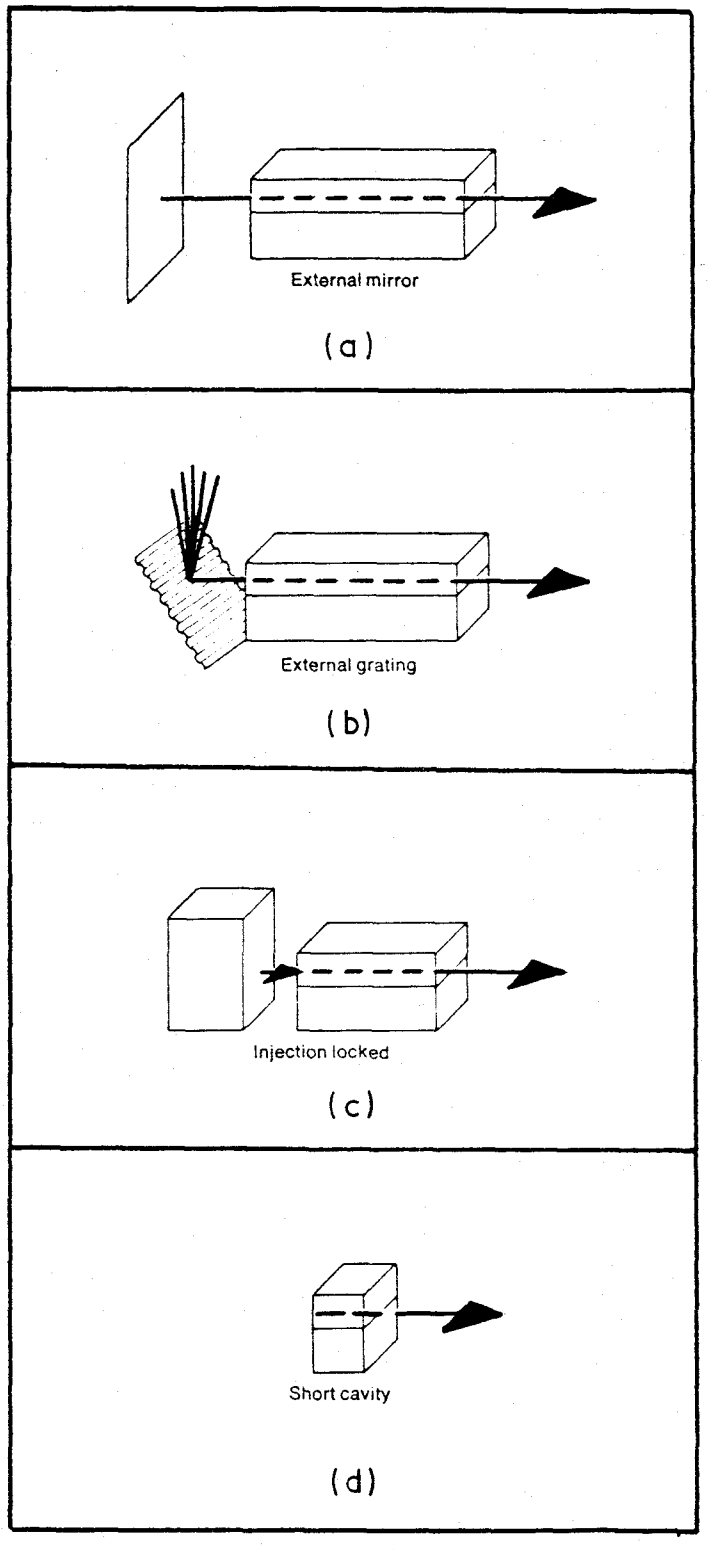

(a) Coupled Cavity laser; (b) Frequency selective feedback; (c) Injection locked laser;
(d) Geometry controlled laser.

Figure 3. Single frequency laser

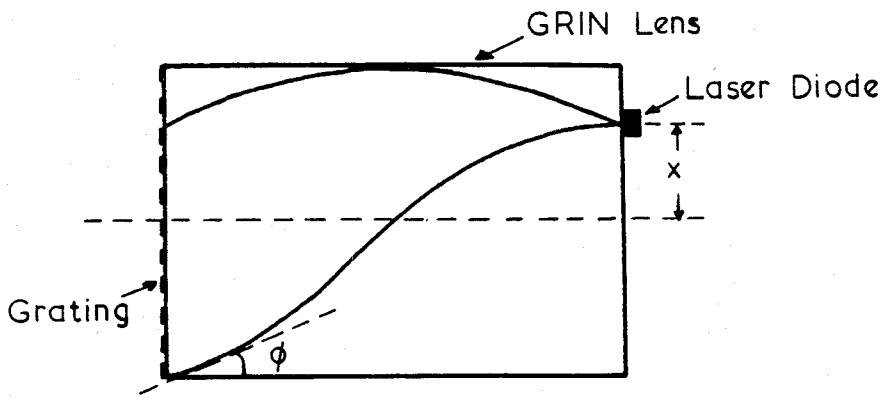

Figure 4. Frequency selective external cavity formed by graded index fibre lens and diffraction grating

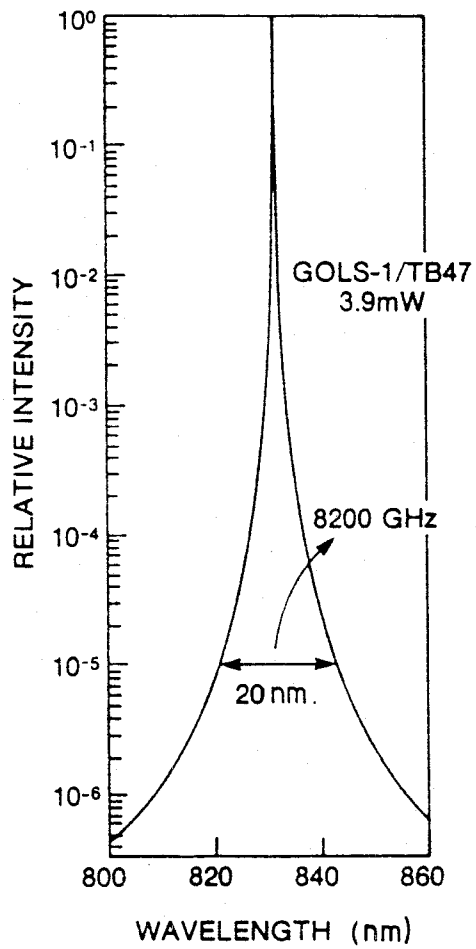

Figure 5. Emission spectrum of general optronics laser diode GOLS-1/TB47 showing spontaneous emission. Laser output 3.9 mW, spectrometer bandpass 0.1 nm (from reference 1)

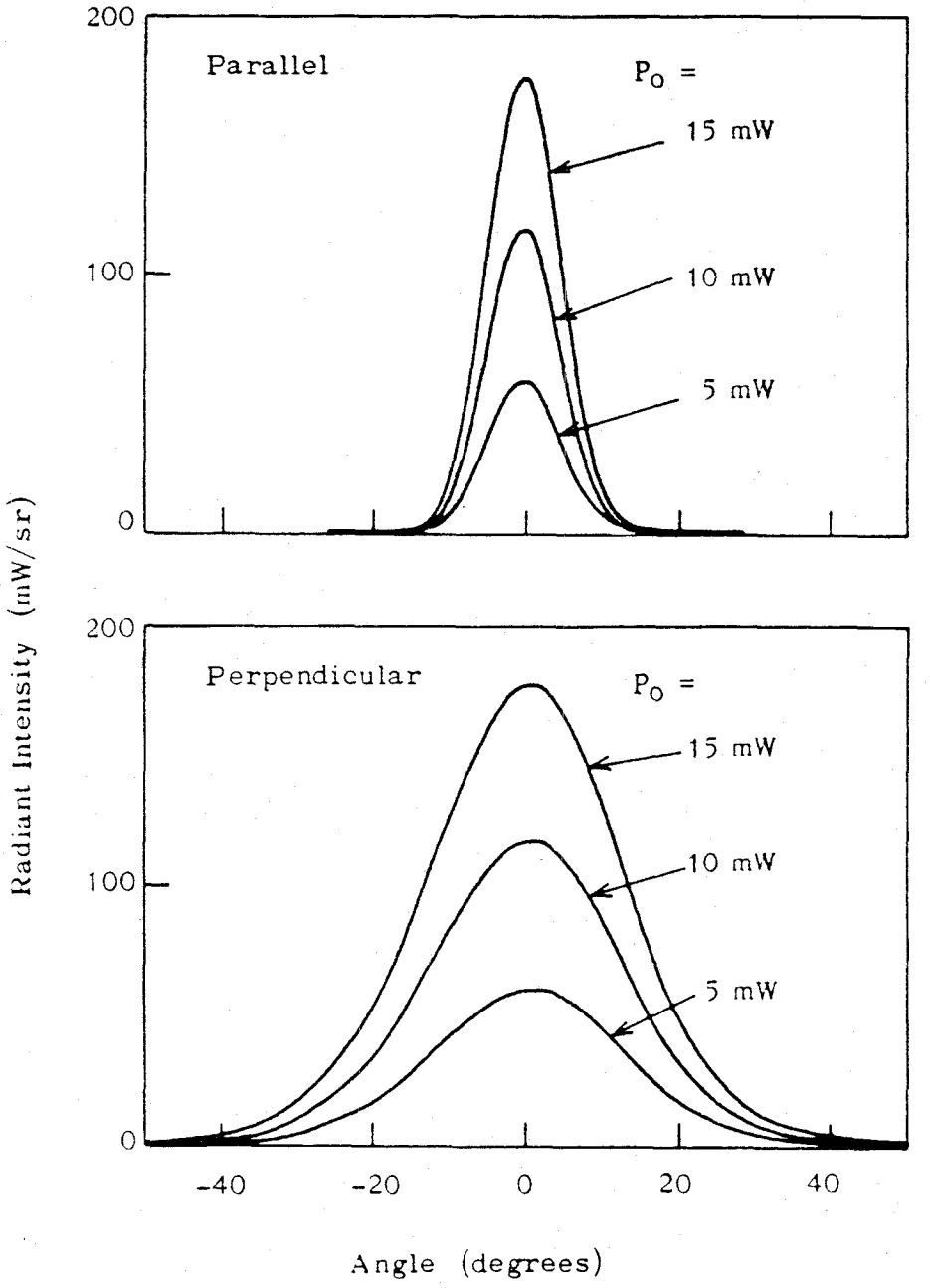

Figure 6. Typical far-field patterns of the HLP-1000 laser diodes parallel and perpendicular to the junction plane(ref.2)

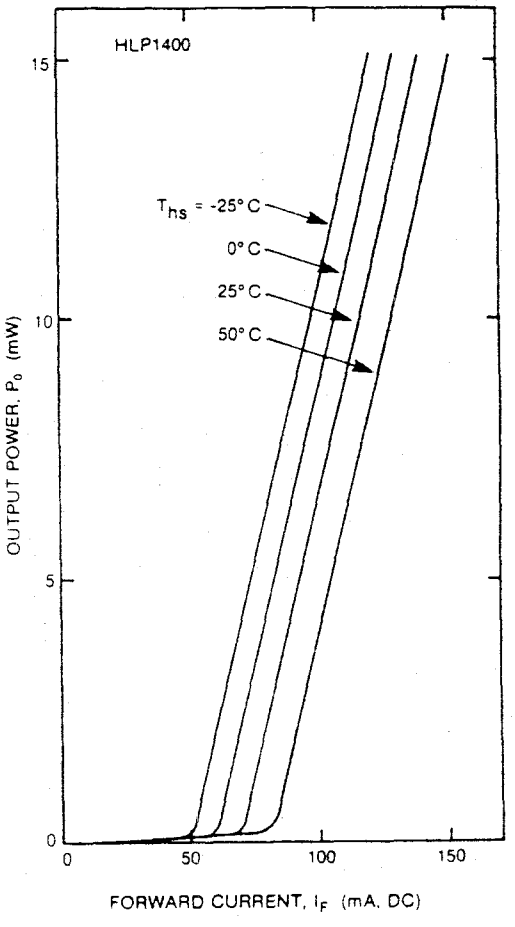

Figure 7. Typical light versus current characteristics for the Hitachi HLP-1000 series laser diodes(ref.2)

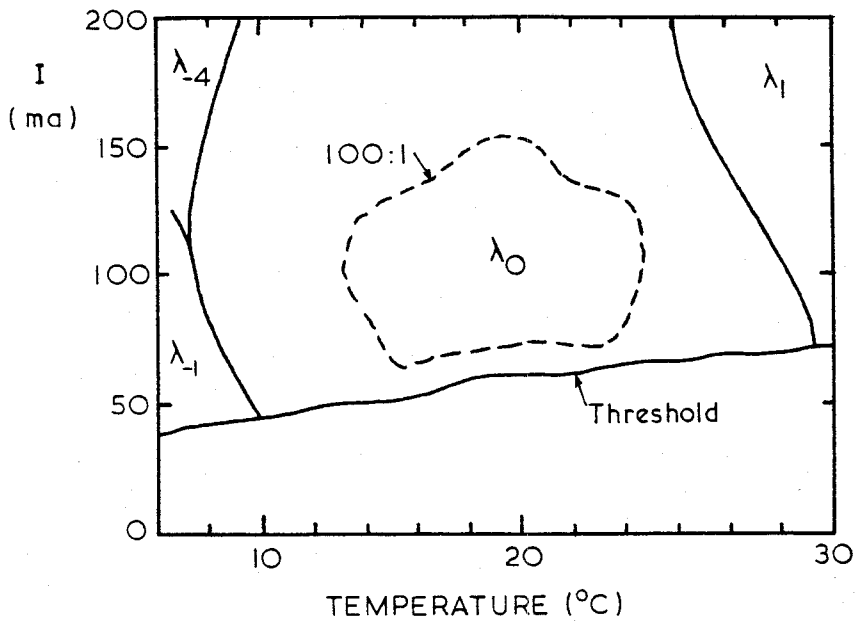

Figure 8. Dominant lasing mode dependence on temperature and current for C^3 laser diode. Solid lines indicate mode hop boundaries; dashed line indicates better than 100:1 peak-to-sidelobe region (from reference 12)

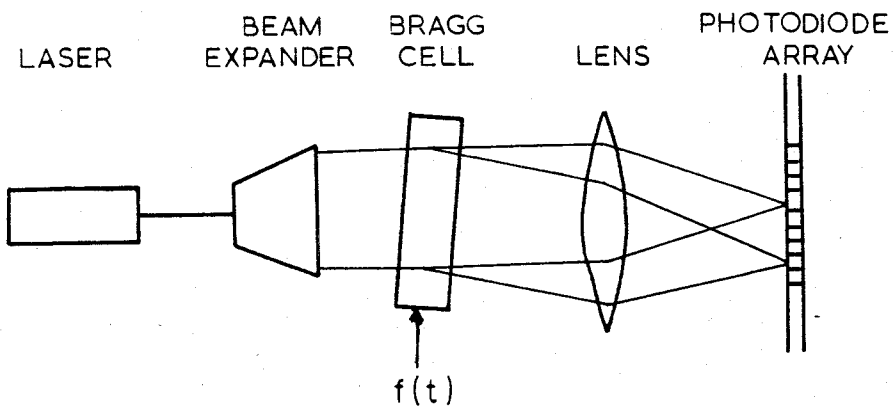

Figure 9. Basic acousto-optic spectrum analyser

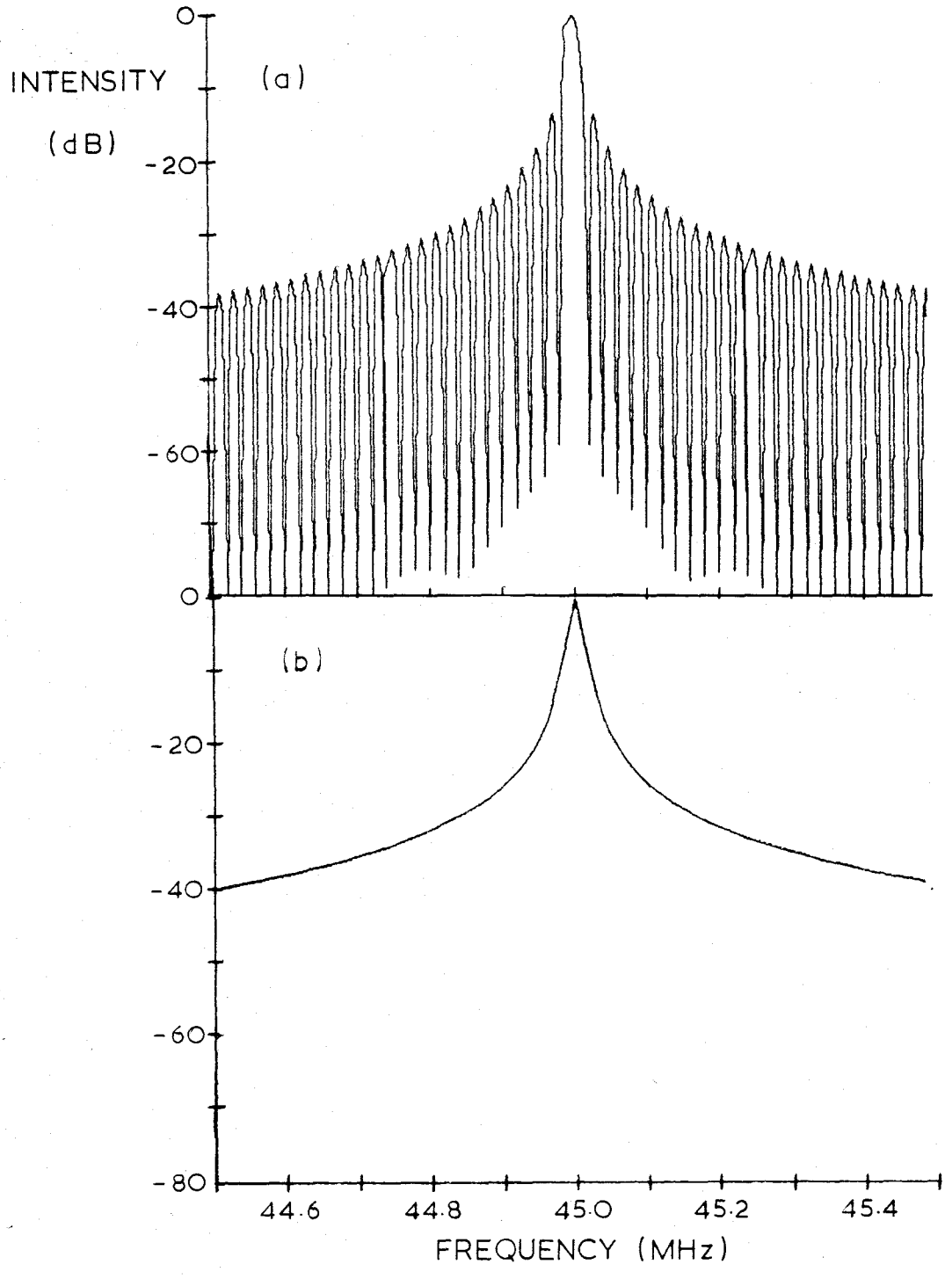

(a) no pixel averaging

(b) pixel averaging, 20 kHz resolution, included

Figure 10. Model output, CW signal, 45 MHz, flat aperture weighting, 50 μs duration

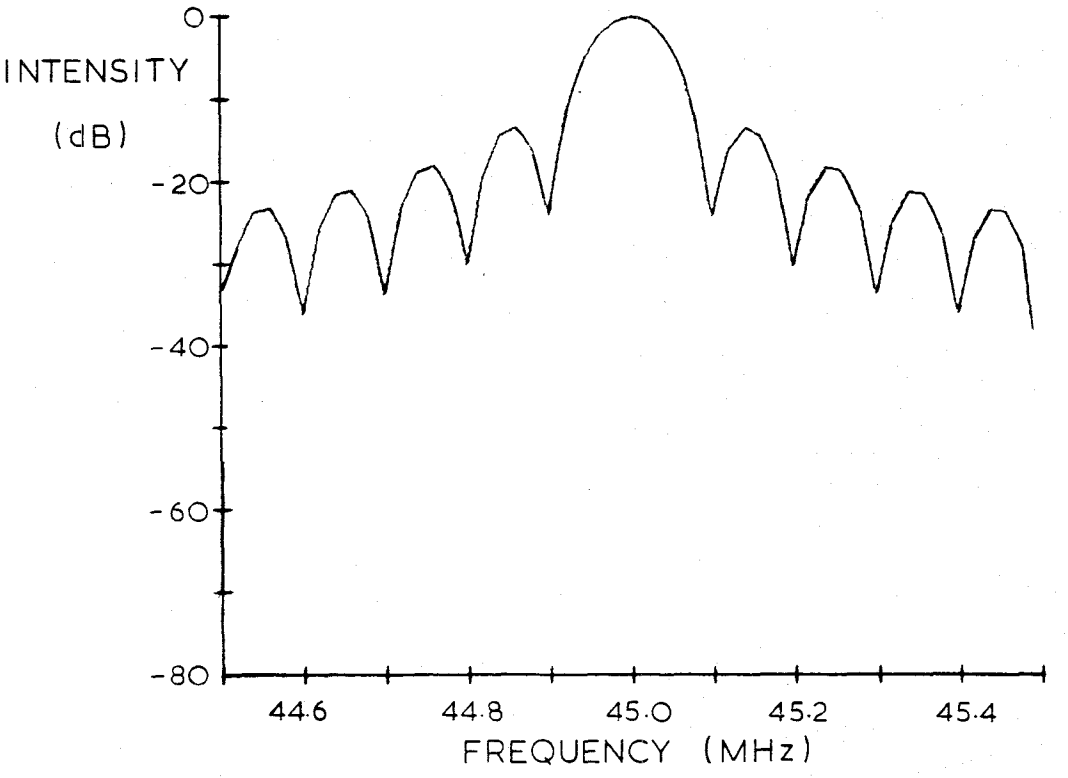

Figure 11. Model output, CW signal, 45 MHz, flat aperture weighting, 10 μs duration

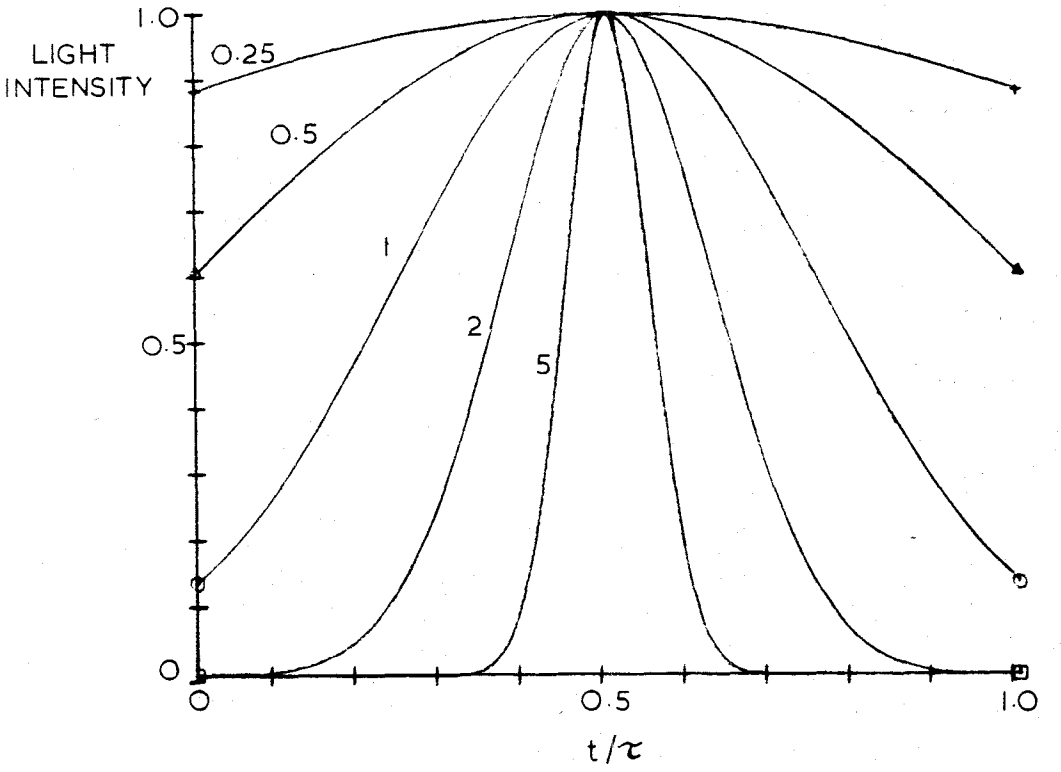

Figure 12. Gaussian laser intensity profiles for various values of the parameter T

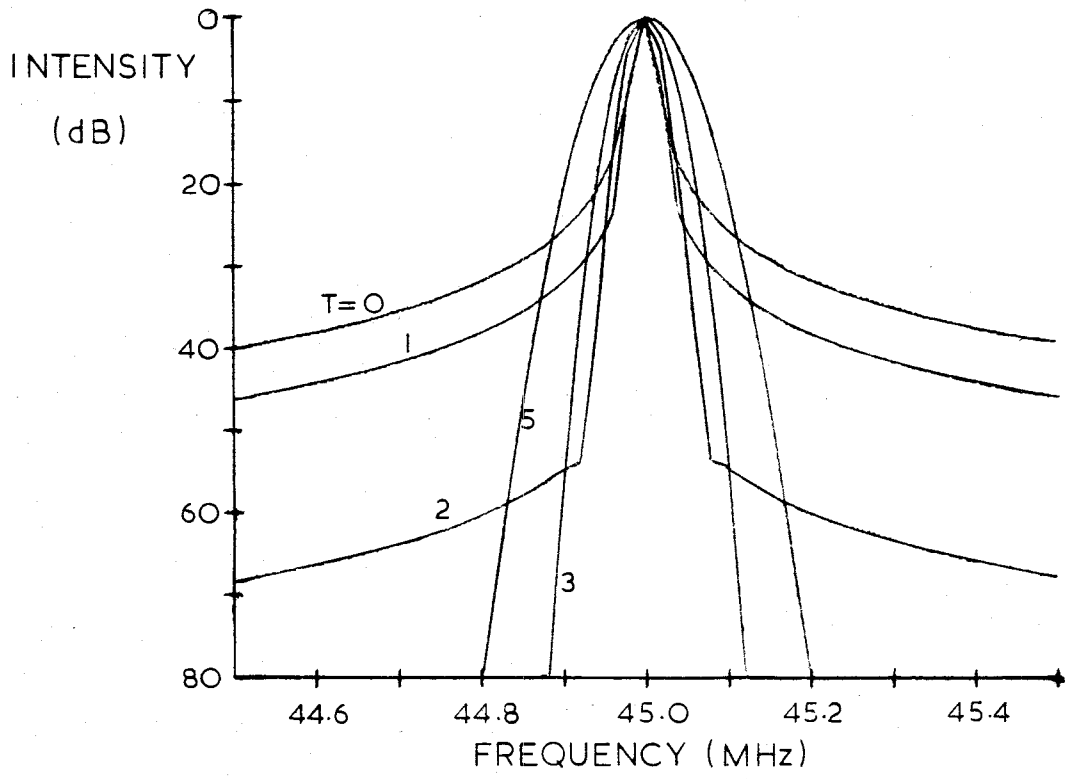

Figure 13. Normalised AO spectrum analyser performance with Gaussian aperture weighting for various Gaussian parameter values. Input: CW signal, 45 MHz

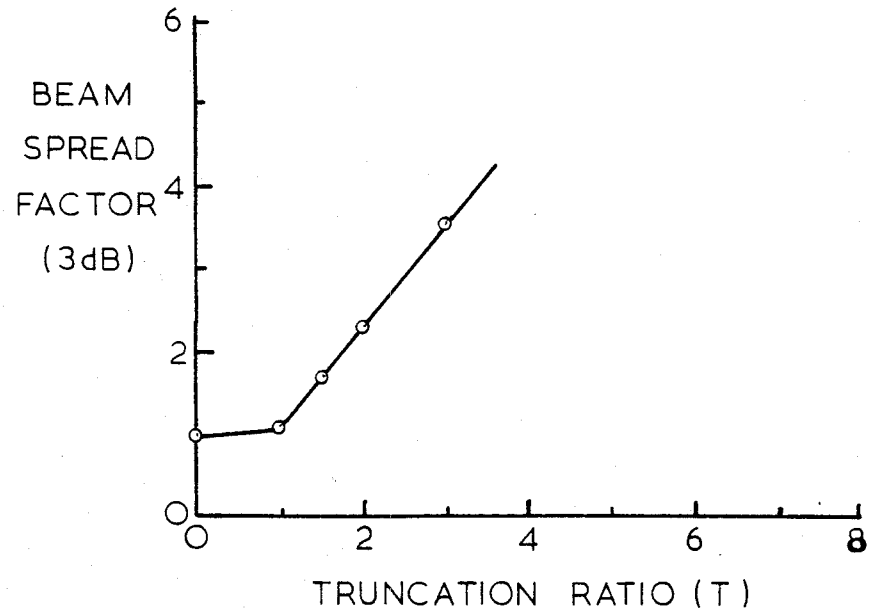

Figure 14. Beam spread factor (3 dB) as a function of Gaussian beam truncation ratio T. Input: CW signal, 45 MHz

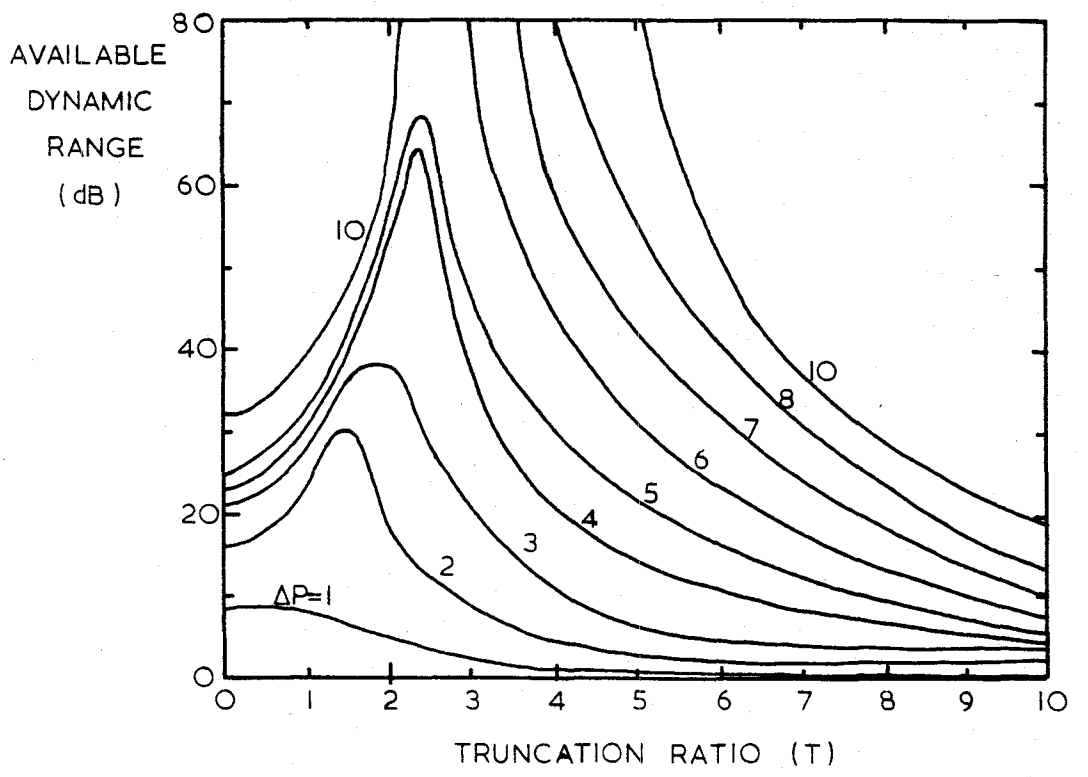

Figure 15. Available dynamic range as a function of Gaussian beam truncation ratio T for various pixel separations from "wanted" frequency pixel. Input: CW signal, 45 MHz

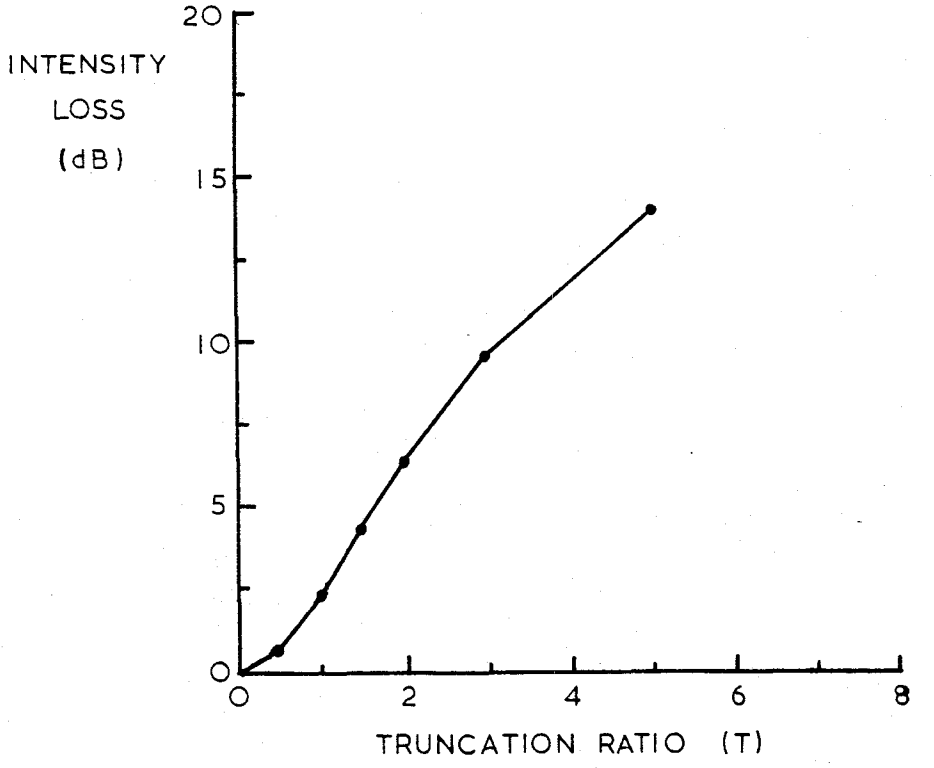

Figure 16. Intensity loss with respect to uniform aperture illumination as a function of the Gaussian beam truncation ratio T. Input: CW signal, 45 MHz

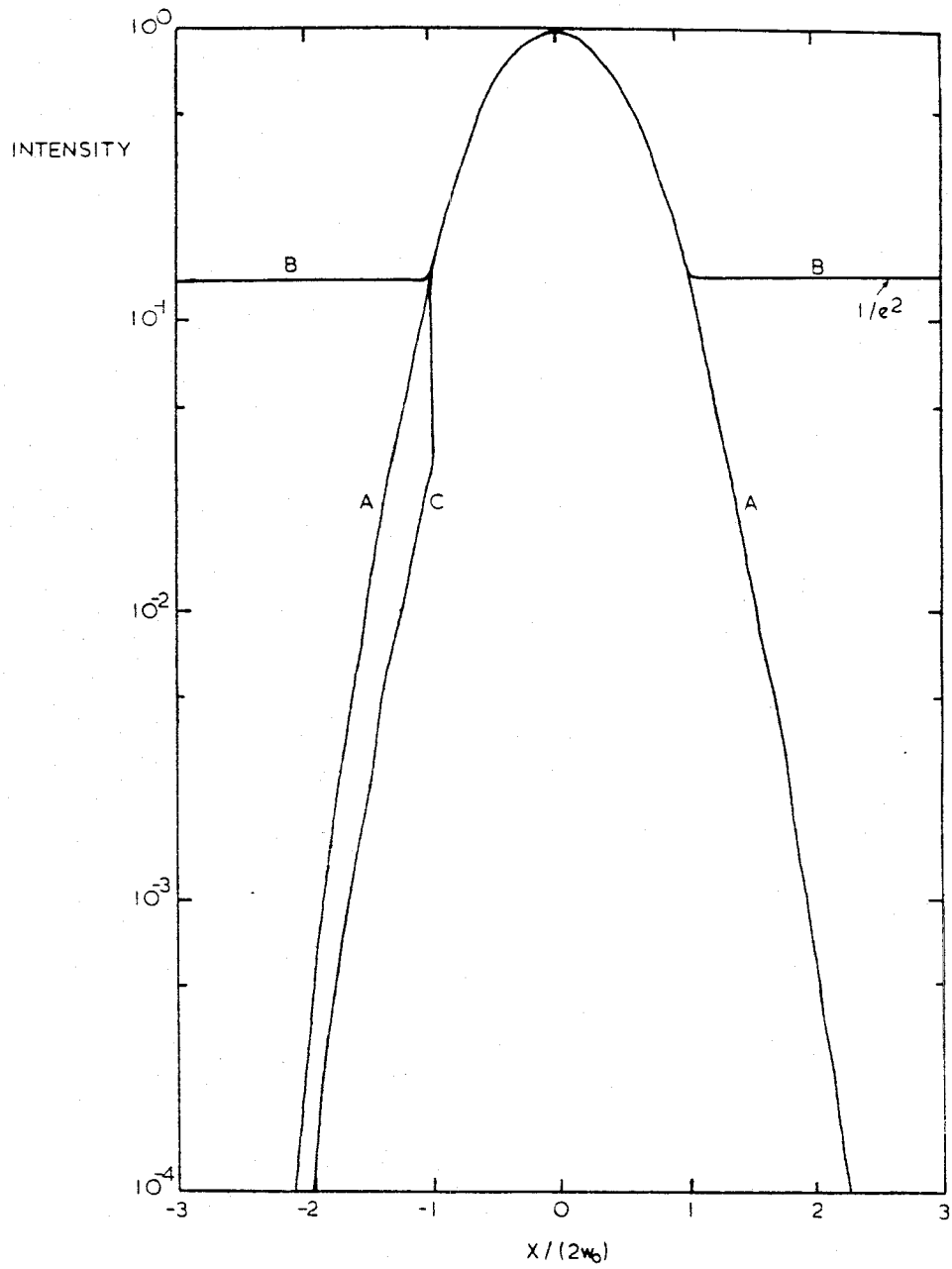

Figure 17. Intensity profiles used to test effect of variations from Gaussian

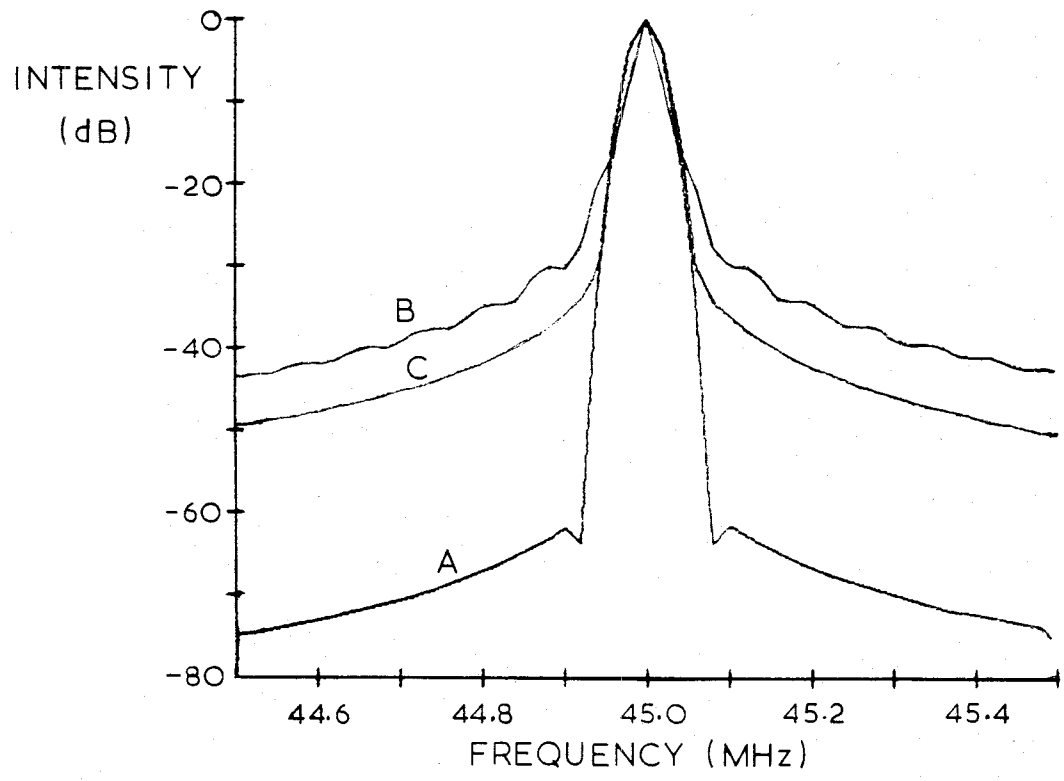

Figure 18. Model output, CW signal, 45 MHz, aperture intensity weighting curves A, B and C of figure 17

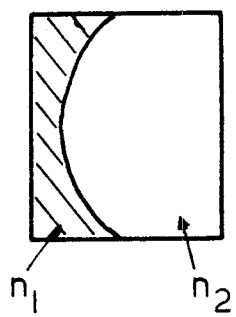

Figure 19. Beam apodisation device

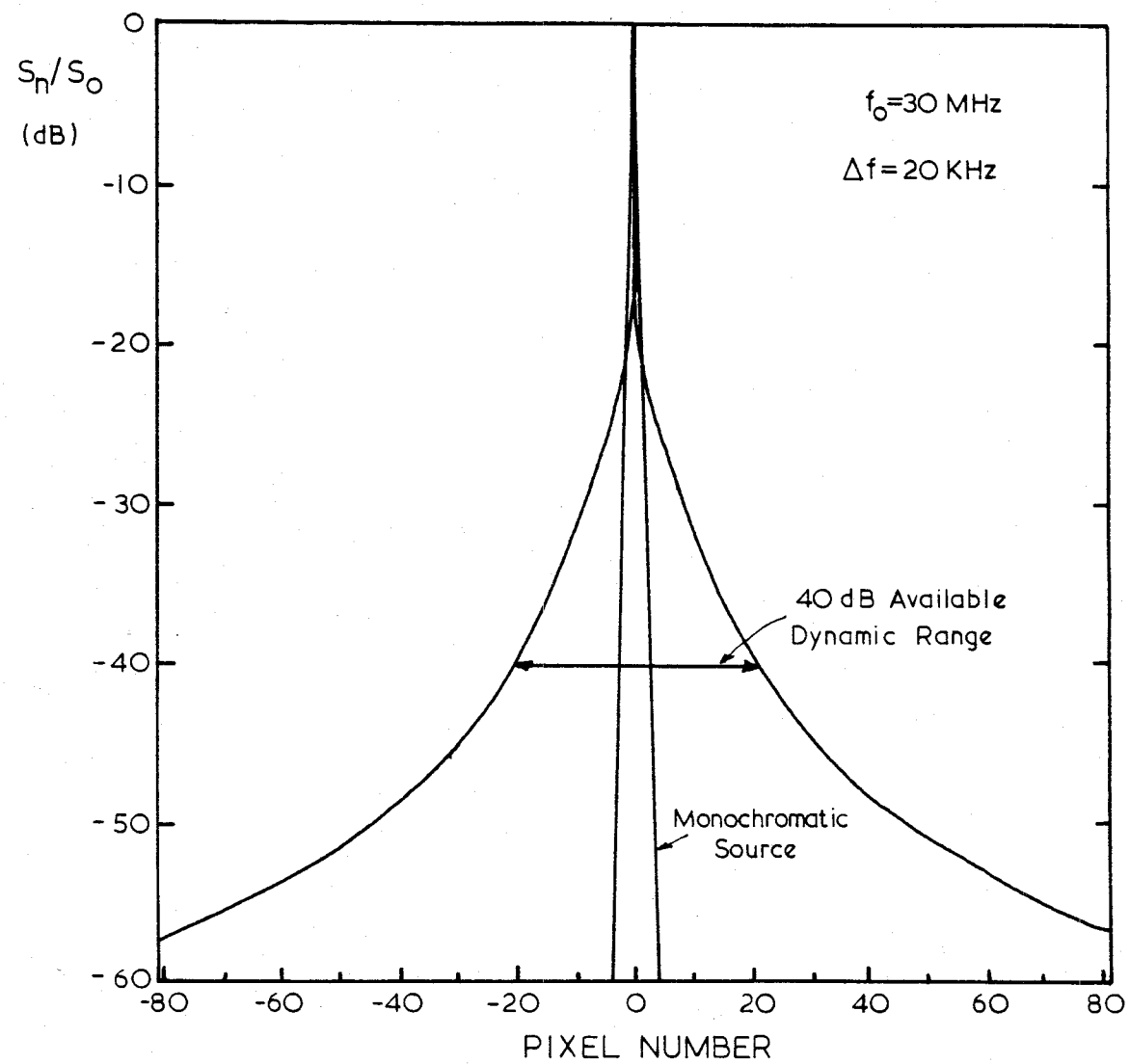

Figure 20. Variation of signal ratio Sn/So with nearest neighbour pixel number for the case of Δf = 20 kHz, f_o = 45 MHz, λ = 830 nm

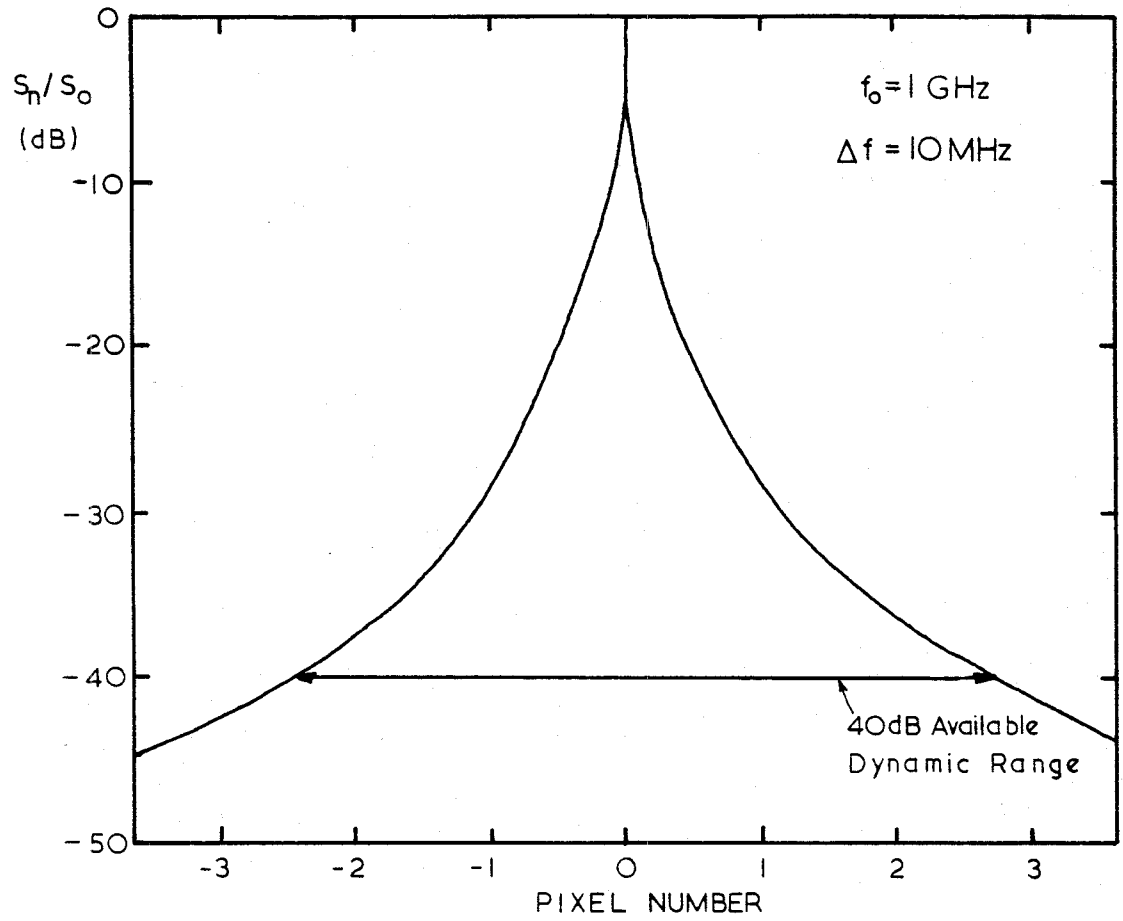

Figure 21. Variation of signal ratio Sn/So with nearest neighbour pixel number for the case of Δf = 10 MHz, f_o = 1 GHz, λ = 830 nm

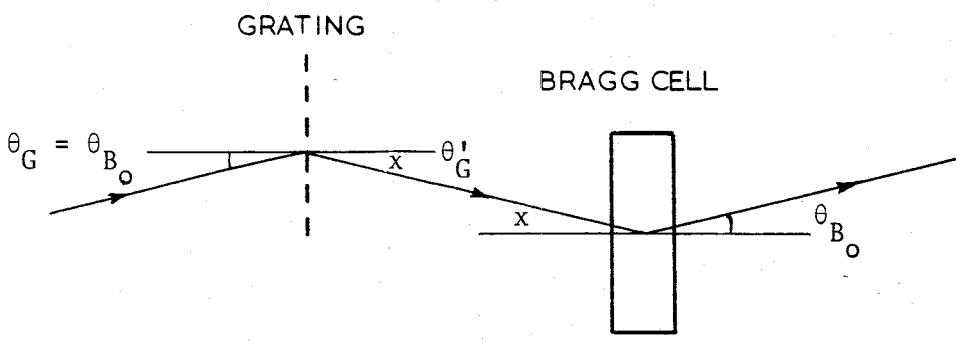

Figure 22. Scheme for chromatic compensation of Bragg cell spectrum analyser

DOCUMENT CONTROL DATA SHEET

Security classification of this page: UNCLASSIFIED

1 DOCUMENT NUMBERS

AR Number: AR-004-264

Series Number: ERL-0346-TM

Other Numbers:

2 SECURITY CLASSIFICATION

a. Complete Document: Unclassified

b. Title in Isolation: Unclassified

c. Summary in Isolation: Unclassified

3 TITLE

USE OF LASER DIODE AS A SOURCE IN A BRAGG CELL SPECTRUM ANALYSER

4 PERSONAL AUTHOR(S):

C.I. Chessell

5 DOCUMENT DATE:

August 1985

6 6.1 TOTAL NUMBER OF PAGES 31

6.2 NUMBER OF REFERENCES: 16

7 7.1 CORPORATE AUTHOR(S):

Electronics Research Laboratory

7.2 DOCUMENT SERIES AND NUMBER

Electronics Research Laboratory 0346-TM

8 REFERENCE NUMBERS

a. Task: DST 82/126

b. Sponsoring Agency:

9 COST CODE:

312452/134

10 IMPRINT (Publishing organisation)

Defence Research Centre Salisbury

11 COMPUTER PROGRAM(S) (Title(s) and language(s))

12 RELEASE LIMITATIONS (of the document):

Approved for Public Release

Security classification of this page: UNCLASSIFIED

Security classification of this page: UNCLASSIFIED

13 ANNOUNCEMENT LIMITATIONS (of the information on these pages):

No limitation

14 DESCRIPTORS:

a. EJC Thesaurus Terms: Spectrum analysers; Semiconductor diodes

b. Non-Thesaurus Terms: Laser diodes; Bragg cells

15 COSATI CODES:

14020

16 SUMMARY OR ABSTRACT:
(if this is security classified, the announcement of this report will be similarly classified)

The effects of using a solid state laser diode as the light source in an acousto-optic spectrum analyser are considered. Concentration is on high resolution analysers for use at communications frequencies. Recent developments in laser diode fabrication are summarised; key characteristics limiting performance are the spectral and spatial characteristics of the laser beam. The effects on analyser resolution and dynamic range are modelled and techniques proposed to improve performance.

Security classification of this page: UNCLASSIFIED